

C2

SKIN FRICTION MEASUREMENTS AT TRANSONIC MACH NUMBERS



Charles L. Smith
ARO, Inc.

October 1979

Final Report for Period 13-15 August 1979

Approved for public release; distribution unlimited.

Property of U. S. Air Force
AEDC LIBRARY
F40600-77-C-0003

PROPERTY OF U. S. AIR FORCE
AEDC TECHNICAL LIBRARY
ARNOLD AFB, TN 37389

**ARNOLD ENGINEERING DEVELOPMENT CENTER
ARNOLD AIR FORCE STATION, TENNESSEE
AIR FORCE SYSTEMS COMMAND
UNITED STATES AIR FORCE**

NOTICES

When U. S. Government drawings, specifications, or other data are used for any purpose other than a definitely related Government procurement operation, the Government thereby incurs no responsibility nor any obligation whatsoever, and the fact that the Government may have formulated, furnished, or in any way supplied the said drawings, specifications, or other data, is not to be regarded by implication or otherwise, or in any manner licensing the holder or any other person or corporation, or conveying any rights or permission to manufacture, use, or sell any patented invention that may in any way be related thereto.

References to named commercial products in this report are not to be considered in any sense as an endorsement of the product by the United States Air Force or the Government.

APPROVAL STATEMENT

This report has been reviewed and approved.



GREGORY COWLEY, 1st Lt, USAF
Test Director, PWT Division
Directorate of Test Operations

Approved for publication:

FOR THE COMMANDER


JAMES D. SANDERS, Colonel, USAF
Deputy for Operations

UNCLASSIFIED

CONTENTS

	<u>Page</u>
NOMENCLATURE	3
1.0 INTRODUCTION	6
2.0 APPARATUS	
2.1 Test Facility	6
2.2 Test Article	7
2.3 Instrumentation	7
3.0 TEST DESCRIPTION	
3.1 Test Conditions and Procedures	8
3.2 Data Reduction Technique	8
3.3 Uncertainty of Measurements	10
4.0 DATA PACKAGE PRESENTATION	10
REFERENCES	10

ILLUSTRATIONS

Figure

1. Model Installation	12
2. Equivalent Body of Revolution Installed in Tunnel 16T	13
3. Test Article and Dimensions	14
4. Test Article Cross-Sectional Area Distribution	15
5. Preston Tube and Boundary-Layer Rake Arrangement and Dimensions	16
6. Construction Details of Embedded Wire Gage . .	17
7. Estimated Uncertainties in Wind Tunnel Parameters	18

	<u>Page</u>
TABLES	
1. Pressure Orifice Locations	19
2. Locations of Wire Gages, Preston Tubes, Boundary-Layer Rakes, and Thermocouples . . .	22
3. Measurement Uncertainties	23
4. Test Program Summary	24
5. Summary of Test Data	25
6. Nomenclature for Summary of Test Data	26
APPENDIX	
WIRE GAGE DATA REDUCTION EQUATIONS	28

NOMENCLATURE

A	Slope of calibration curve for wire gage, watts/ohm
A_i	Surface area between wire gage locations, ft^2
A/AMAX	Ratio of model cross-sectional area to the model's maximum cross-sectional area (1.4243 ft^2)
B	Power loss at zero shear stress for wire gage, watts/ohm
CA	Balance measured total drag coefficient, $FA/Q(S)$
CAPAT	Integrated pressure force coefficient of after-body ($X/L = 0.505$ to $X/L = 1.0$), positive aft
CAPFT	Integrated pressure force coefficient of fore-body ($X/L = 0.505$ to $X/L = 1.0$), positive aft
CAPT	Total integrated pressure force coefficient including cavity pressure contribution, positive aft, $CAPFT + CAPAT - CCAV$
CCAV	Model cavity pressure force coefficient, positive forward, $FCAV/Q(S)$
CFB	Skin friction drag coefficient calculated from balance and pressure data, $CA - CAPT$
CFG	Skin friction drag coefficient calculated from integrated wire gage data, $SF/Q(S)$
CFGAGE	Local skin friction coefficient, $SFGAGE/Q$
COEF	Model surface pressure coefficient, $[144(\text{PRES}) - P]/Q$
FA	Balance measured axial force, positive aft, lb
FCAV	Model cavity pressure force, positive forward, lb
IGAGE	Current through the wire gage, amperes
ISR	Gage power loss per unit change in resistance, $(VGAGE)(IGAGE)/(RHOT - RCOLD)$, watts/ohm
KA	Slope of temperature versus resistance curve for each wire gage, $^{\circ}\text{F}/\text{ohm}$

KB	Temperature required for zero wire gage resistance, °F
M	Free-stream Mach number
MS	Model station in inches aft of the nose
MU	Local viscosity based on TG, lb-sec/ft ²
P	Free-stream static pressure, psfa
PRES	Model surface static pressure, psia
PXXX	Model surface static pressure selected for the calculation of RHO for each gage, psia
Q	Free-stream dynamic pressure, psf
R	Model radius, in.
RCOLD	Resistance of the wire gage at the model surface temperature, ohm
REX10-6	Free-stream unit Reynolds number x 10 ⁻⁶ , 1/ft
RHO	Local flow density evaluated at local static pressure and TG, lbm/ft ³
RHOT	Resistance of the wire gage at operating temperature, ohm
RUN NUMBER	A data subset containing variation of only one independent parameter
S	Model reference area (maximum cross-sectional area), 1.4243 ft ²
SF	Integrated wire gage friction force, lb
SFGAGE	Skin friction per unit area for each wire gage, lb/ft ²
TAP	Pressure orifice number
TG	Wire gage operating temperature, °R
TTR	Free-stream total temperature, °R
T2-14	Model surface temperature, °R
VGAGE	Voltage across the wire gage, volts

X/L Model station in inches aft of nose divided by model length (130,053 in.)

θ Radial position on the model measured from the top row of pressure orifices, positive clockwise looking upstream, deg

θ_i Angle of the model surface at each wire gage location relative to the model axis, deg

1.0 INTRODUCTION

The work reported herein was conducted at the Arnold Engineering Development Center (AEDC), Air Force Systems Command (AFSC), at the request of the AEDC Technology Division (AEDC/DOT), under Program Element 65807F. The test results were obtained by ARO, Inc., AEDC Group (a Sverdrup Corporation Company), operating contractor of AEDC, AFSC, Arnold Air Force Station, Tennessee. The test was conducted in the Propulsion Wind Tunnel (16T) of the Propulsion Wind Tunnel Facility (PWT) August 13 through August 15, 1979, under ARO Project Number P41T-A2.

The objective of the test was to evaluate a method of measuring skin friction on wind tunnel models in transonic flow using embedded wire gages. A body of revolution was tested with embedded wire gages, surface pressure orifices, Preston tubes, and boundary-layer rakes at various axial stations on the body. A balance was used to measure the total axial force on the model. The model was tested at 0-deg angle of attack at Mach numbers from 0.6 to 1.5 and unit Reynolds numbers from $1.5 \times 10^6/\text{ft}$ to $5.0 \times 10^6/\text{ft}$.

The purpose of this report is to document the test and to describe the test parameters. The report provides information to permit use of the data, but does not include any data analysis, which is beyond the scope of this report.

The final data from this test have been transmitted to AEDC/DOT, Arnold Air Force Station, Tennessee 37389. Requests for these data should be addressed to AEDC/DOT. A copy of the final data is on microfilm at AEDC.

2.0 APPARATUS

2.1 TEST FACILITY

The AEDC Propulsion Wind Tunnel (16T) is a variable density, continuous-flow tunnel capable of being operated at Mach numbers from 0.2 to 1.5 and stagnation pressures from 120 to 4,000 psfa. The maximum attainable Mach number can vary slightly depending upon the tunnel pressure ratio requirements with a particular test installation. The maximum stagnation pressure attainable is a function of Mach number and available electrical power. The tunnel stagnation temperature can be varied from about 80 to 160°F depending upon the available cooling water temperature. The test section is 16 ft square by 40 ft long and is enclosed by

60-deg inclined-hole perforated walls of six-percent porosity. The general arrangement of test section with the test article installed is shown in Fig. 1. Additional information about the tunnel, its capabilities and operating characteristics is presented in Ref. 1.

2.2 TEST ARTICLE

The axisymmetric equivalent body of revolution represented the cross-sectional area distribution of a typical twin jet fighter. The sting-supported model is shown installed in the 16T test section in Fig. 2, and a sketch with pertinent dimensions is presented in Fig. 3. The cross-sectional area distribution is plotted in Fig. 4.

2.3 INSTRUMENTATION

The model was instrumented to determine skin friction by several methods. A six-component strain gage balance was used to measure the total drag force on the model. Integrated pressure drag was determined from 176 model surface static and 4 cavity pressures. Additional pressure measurements on the model included 9 Preston tubes and 4 eleven-probe boundary-layer rakes whose arrangement and dimensions are presented in Fig. 5. All model pressures were measured with a six module scanning-valve system using 15-psid transducers. The 48-port valves were controlled by a facility computer in a step-pause mode which monitored each pressure to ensure stabilization before advancing to the next port. Pressure orifice locations are presented in Table 1 followed by Preston tube and boundary-layer rake locations in Table 2.

The model was originally configured with 40 embedded wire skin friction gages (wire gages) and 14 copper-constantan thermocouples (31 wire gages and 12 thermocouples were eventually used for data reduction). Model locations for the wire gages and thermocouples are presented in Table 2. The wire gages were calibrated to measure skin friction as a function of the power required to replace convective heat losses from a small wire exposed to the local flow field. A sketch showing construction details of the wire gage is presented in Fig. 6. The thermocouples measured local skin temperature and were used to verify wire gage readings and to reduce Preston tube data.

3.0 TEST DESCRIPTION

3.1 TEST CONDITIONS AND PROCEDURES

Data were obtained at free-stream Mach numbers from 0.6 to 1.5 and unit Reynolds numbers from $1.5 \times 10^6/\text{ft}$ to $5.0 \times 10^6/\text{ft}$. After stabilizing, the model surface temperature was obtained for each wire gage by applying a very low current and these values were stored for later calculations. Then, the current to each gage was adjusted to provide a pre-selected increase in gage temperature, and two steady-state points were obtained. The test matrix was accomplished with and without Preston tubes and boundary-layer rakes installed. Wind tunnel specific humidity and total temperature were varied for the latter configuration which represented primary balance and wire gage data.

3.2 DATA REDUCTION TECHNIQUE

The skin friction drag coefficient was obtained from the balance and pressure data by subtracting the total integrated pressure force coefficient from the balance measured drag coefficient. Forebody pressure integrations were performed over the body of revolution from $X/L = 0.0$ to $X/L = 0.505$ (axial location of maximum cross-sectional area) and afterbody integrations from $X/L = 0.505$ to $X/L = 1.0$. The integrations were obtained by summing the products of the average pressure coefficients multiplied by the axial projections of the areas between succeeding pressure orifices. The pressure level was assumed uniform around the body or averaged where more than one orifice existed at each axial station. The stagnation pressure coefficient and the model cavity pressure coefficient were averaged with the first and last pressure coefficients, respectively. The stagnation pressure coefficient used in the integration was based on the stagnation pressure behind a normal shock wave for the supersonic test conditions. The integrated force coefficients were based on the model's maximum cross-sectional area (1.4243 ft^2). The total integrated pressure force coefficient includes the cavity pressure force coefficient which was based on the model's maximum cross-sectional area and free-stream dynamic pressure,

$$\text{CAPT} = \text{CAPFT} + \text{CAPAT} - \text{CCAV}.$$

The parameter CFRM was based on the Frankl-Voishel empirical flat plate, skin friction drag equation for fully turbulent flow (Eq. 27.66a, Ref. 2). This empirical coefficient was calculated from Mach number and Reynolds number and multiplied by the ratio of the model's wetted area divided by maximum cross-sectional area.

Embedded wire gage data consisted of the voltage across the gage and the current through the gage. These values were used to calculate the power required to maintain the operating temperature of the gage at a preselected value. For a gage with a small streamwise dimension, the power required per degree of temperature rise (or per ohm rise in resistance) of the gage is linearly related to the cube root of the local flow density times the local wall shear stress divided by the local viscosity squared. (The local density and viscosity are evaluated at the operating temperature of the gage as in Ref. 3.) The slope and intercept of the curve were determined by calibration of the individual gages at known values of shear stress. Pretest calibrations were performed in the Acoustic Research Tunnel (ART) using a Preston tube as a calibration standard. However, the transfer of the gages from the ART to the model altered the operating characteristics of the embedded wire gages in a random fashion. Therefore, new calibration coefficients were derived by using the Preston tube data obtained during the initial testing phase at a Mach number of 0.6 and unit Reynolds numbers of 1.5, 2.25, and 3.35×10^6 /ft. The Preston tube data reduction technique presented by J. M. Allen (Ref. 4) was used to obtain values of local shear stress. At the calibration conditions described, excellent agreement was found between the theoretical calculations using the SWIM computer code developed by D. L. Whitfield and the measured Preston tube values. Therefore, the theoretical calculations were used to supply values of shear stress ahead of the first Preston tube and to interpolate between Preston tubes. (The SWIM code assumes turbulent flow from the leading edge of the model, therefore, the gage or gages nearest the nose may be in error if the flow is laminar rather than turbulent.) The calibration constants for each gage were determined by performing a least-squares linear curve fit on the three data points obtained at the calibration conditions. These constants were used to reduce all embedded wire data using the equations presented in the Appendix. The excellent agreement between the measurements and theory at the calibration conditions is the consequence of using the theory to aid in the calibration of the gages and should not be interpreted as support for the theory.

The total skin friction drag was determined by integrating the individual embedded wire skin friction values assuming that the body was perfectly axisymmetric (i.e., at a given axial location, the skin friction is the same at any point around the body). The surface area of the model was divided into bands with an embedded wire gage on the upstream and downstream edge of the band. The average of

the skin friction measured on each edge of the area band was assumed to be the friction force per unit area of the band. The friction force was resolved into a component parallel to the model axis. Each parallel component was multiplied by the fraction of the total area in the corresponding area band, and summed to provide the total integrated skin friction drag force. The equation is presented in the Appendix. The embedded wire gage skin friction drag coefficient was based on the model reference area, S , and free-stream dynamic pressure, Q .

3.3 UNCERTAINTY OF MEASUREMENTS

Uncertainties (combinations of systematic and random errors) of the basic tunnel parameters, shown in Fig. 7, were estimated from repeat calibration of the instrumentation and from the repeatability and uniformity of the test section flow during tunnel calibration. Uncertainties in the instrumentation systems were estimated from repeat calibration of the systems against secondary standards whose uncertainties are traceable to the National Bureau of Standards calibration equipment. The instrument uncertainties are combined using the Taylor series method of error propagation described in Ref. 5 to determine the uncertainties of the reduced parameters shown in Table 3.

4.0 DATA PACKAGE PRESENTATION

A test summary correlating run number with the test conditions is presented in Table 4. A summary of the test data is presented in Table 5 followed by its nomenclature in Table 6. Parameters referred to elsewhere in the report are defined in the nomenclature section of the report. The final data package consists of the tabulated data, installation photographs, and a copy of this report.

REFERENCES

1. Test Facilities Handbook (Eleventh Edition). "Propulsion Wind Tunnel Facility, Vol. 4." Arnold Engineering Development Center, June 1979.
2. Shapiro, A. H. The Dynamics and Thermodynamics of Compressible Fluid Flow. Vol. II, Ronald Press Company, New York, 1954.

3. Murthy, V. S., and Rose, W. C., "Direct Measurements of Wall Shear Stress by Buried Wire Gages in a Shock Wave-Boundary Layer Interaction Region," AIAA Paper 77-691, June 1977.
4. Allen, J. M. "Evaluation of Compressible-Flow Preston Tube Calibrations." NASA TN D-7190, May 1973.
5. Abernethy, R. B. and Thompson, J. W., Jr. "Handbook - Uncertainty in Gas Turbine Measurements." AEDC-TR-73-5 (AD755356), February 1973.

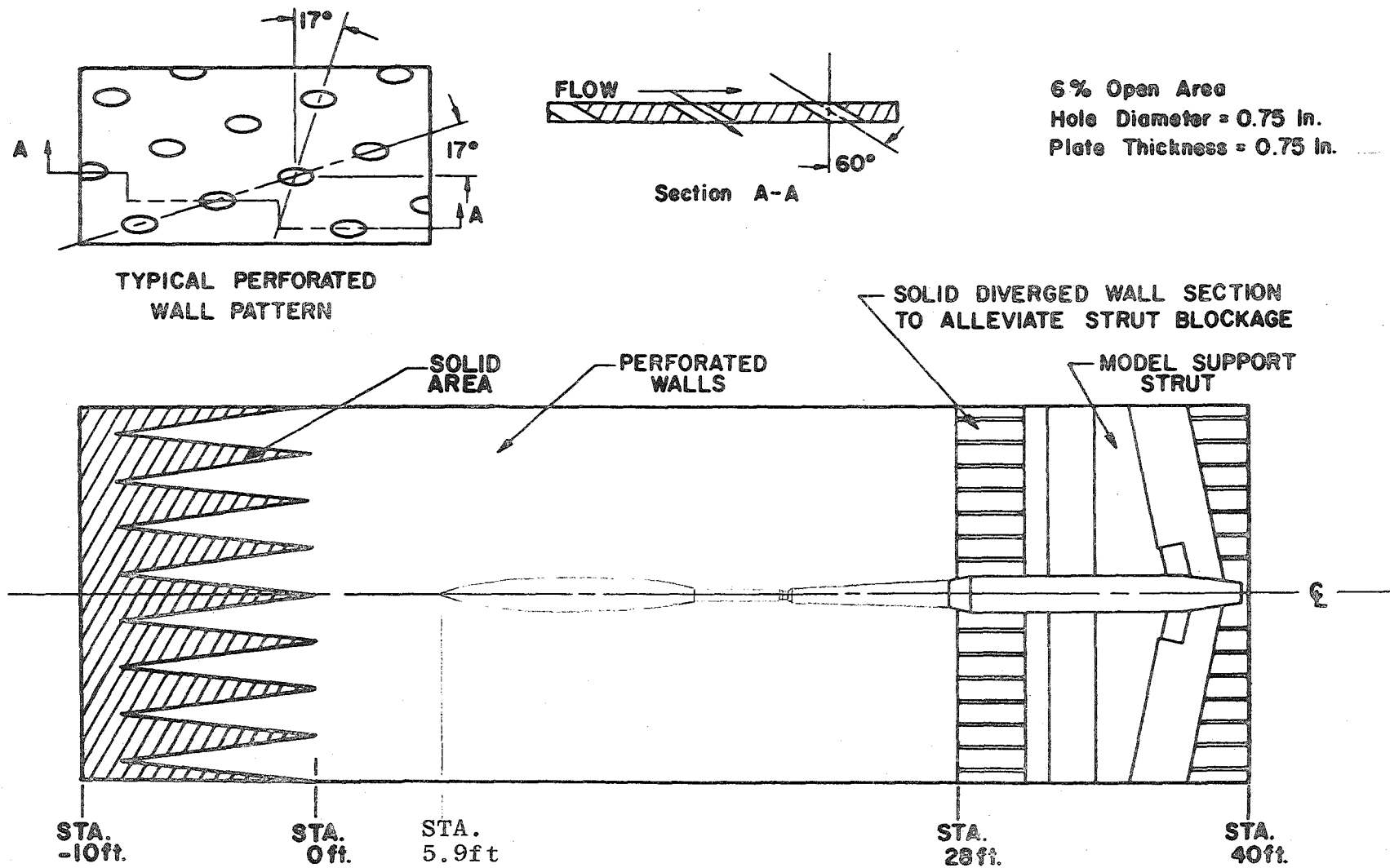


Figure 1. Model Installation

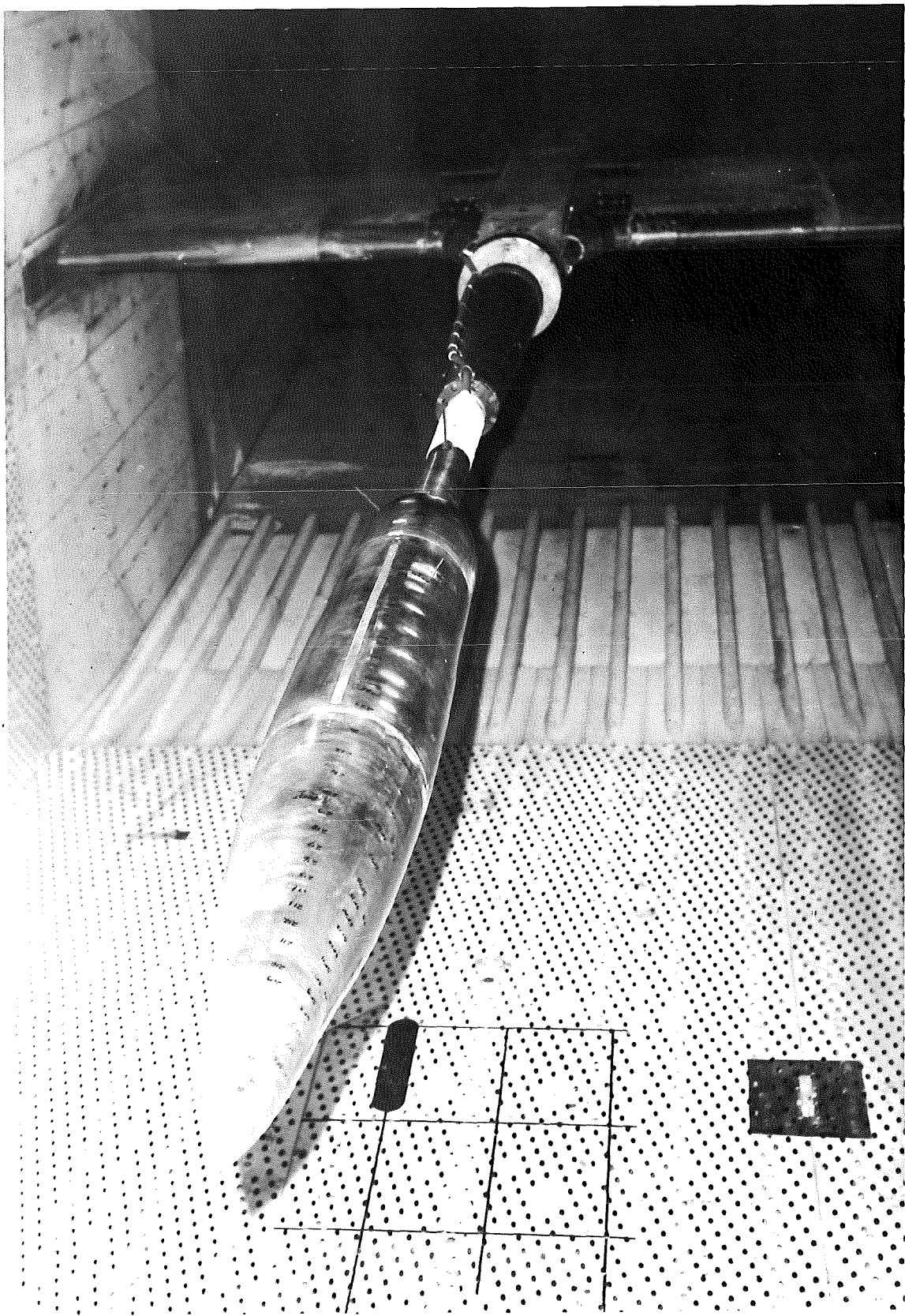


Figure 2. Equivalent Body of Revolution Installed in Tunnel 16T

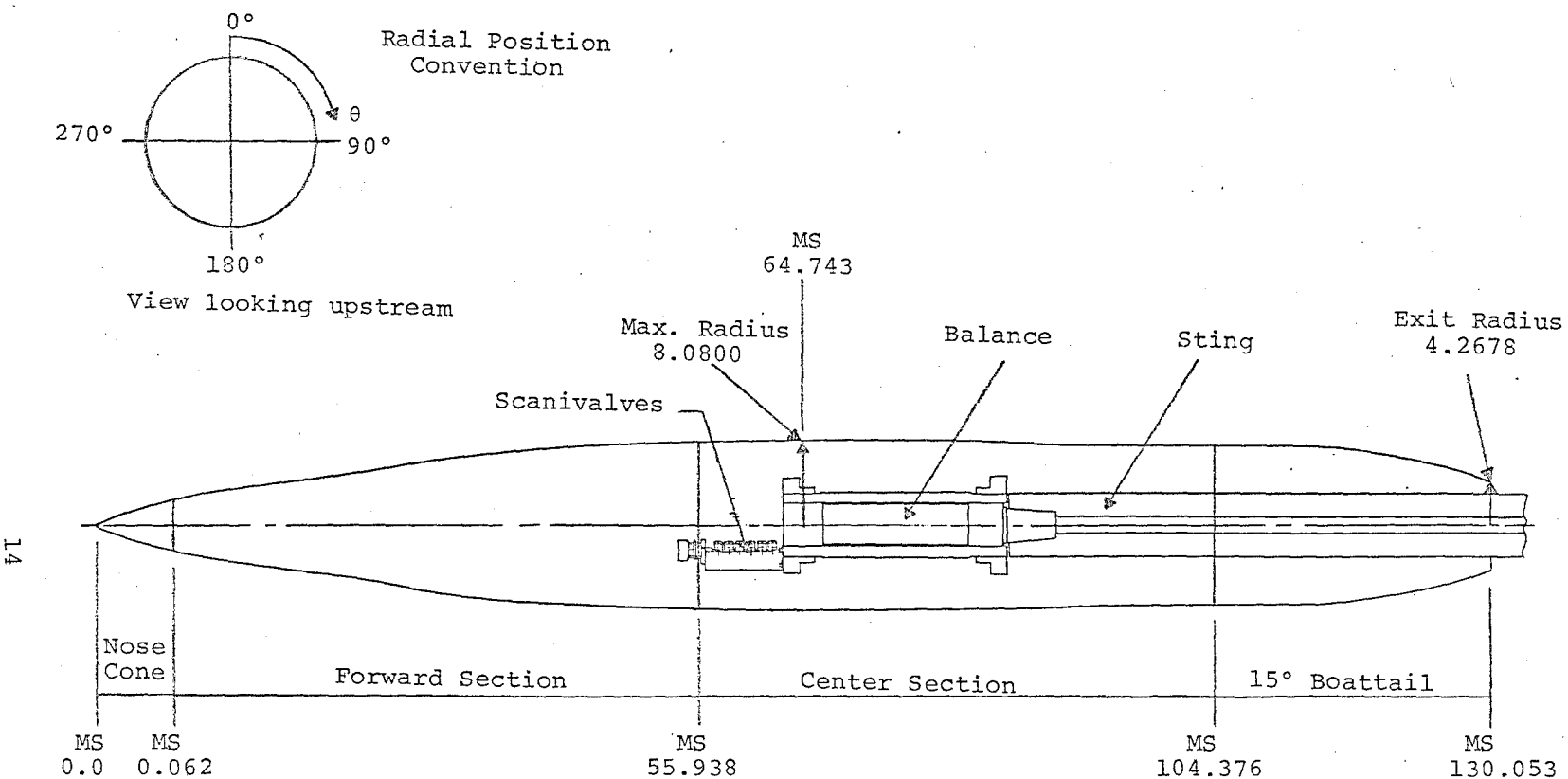


Figure 3. Test Article and Dimensions

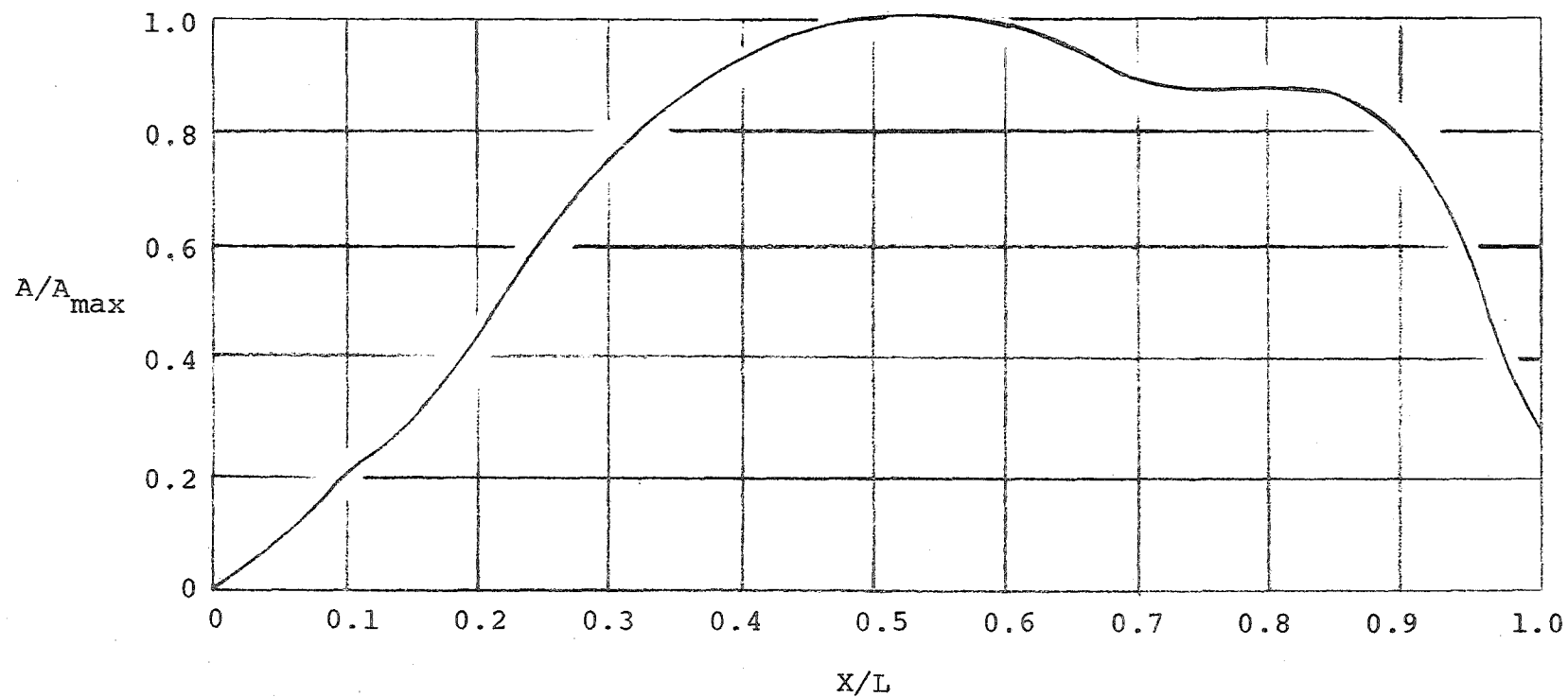
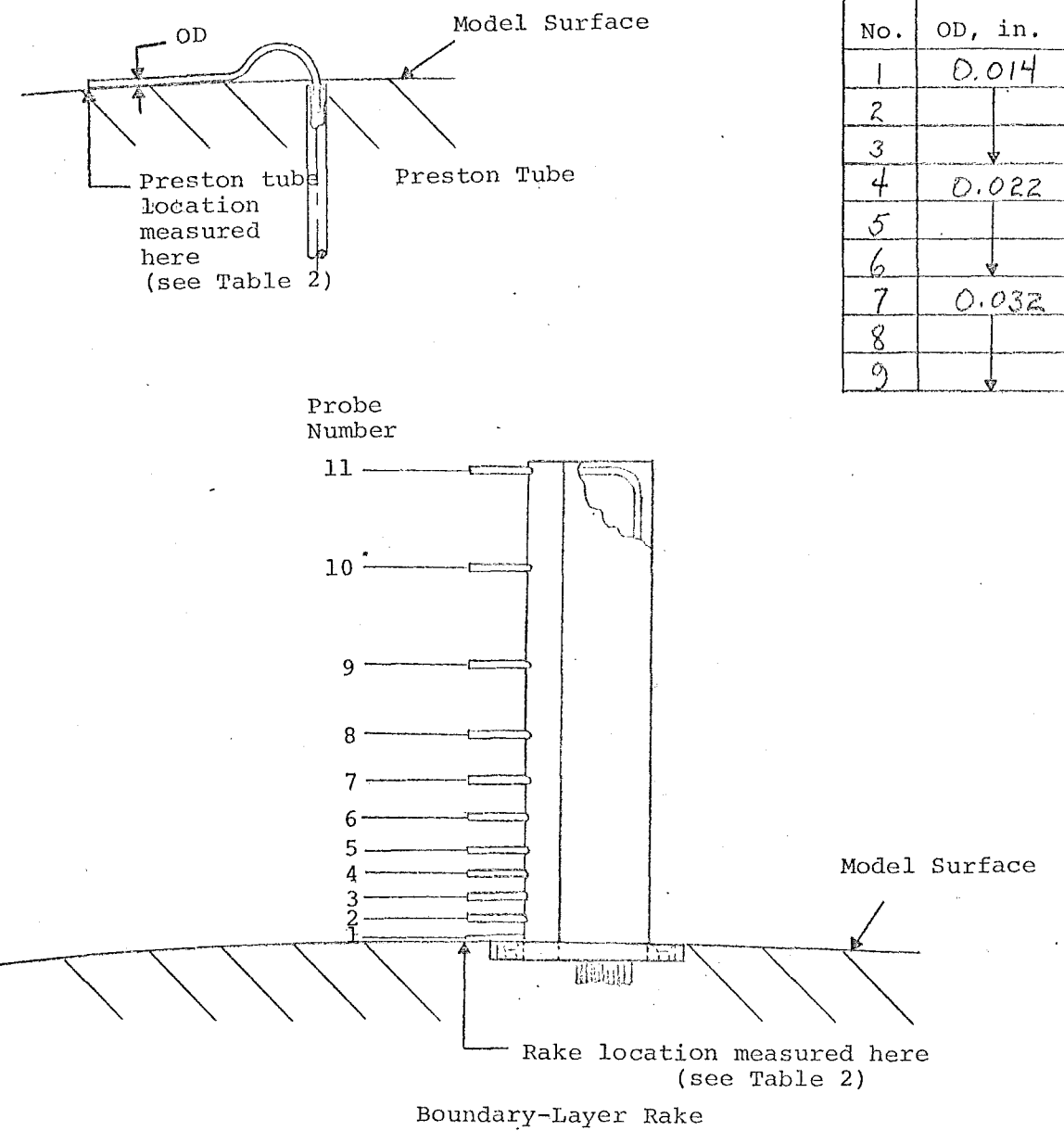


Figure 4. Test Article Cross-Sectional Area Distribution



Distance from Model Surface to Centerline of Probe in Inches

No.	1	2	3	4	5	6	7	8	9	10	11
1	.018	.088	.158	.238	.333	.458	.603	.778	1.053	1.408	1.758
2	.020	.090	.170	.245	.340	.470	.620	.790	1.065	1.425	1.765
3	.020	.085	.165	.245	.350	.465	.615	.795	1.070	1.420	1.765
4	.020	.185	.370	.580	.815	1.070	1.410	1.845	2.470	3.260	4.040

Figure 5. Preston Tube and Boundary-Layer Rake Arrangement and Dimensions

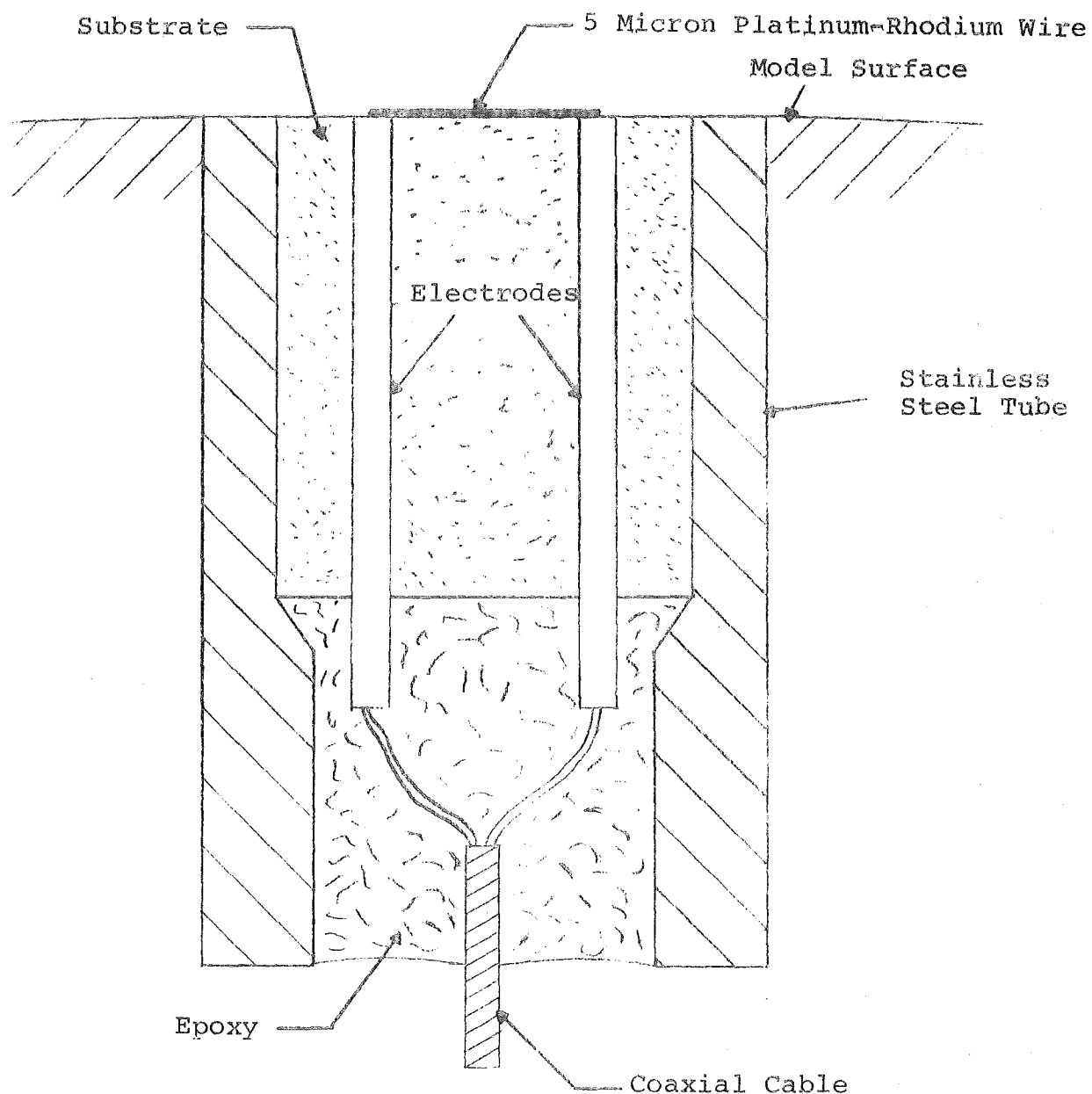


Figure 6. Construction Details of Embedded Wire Gage

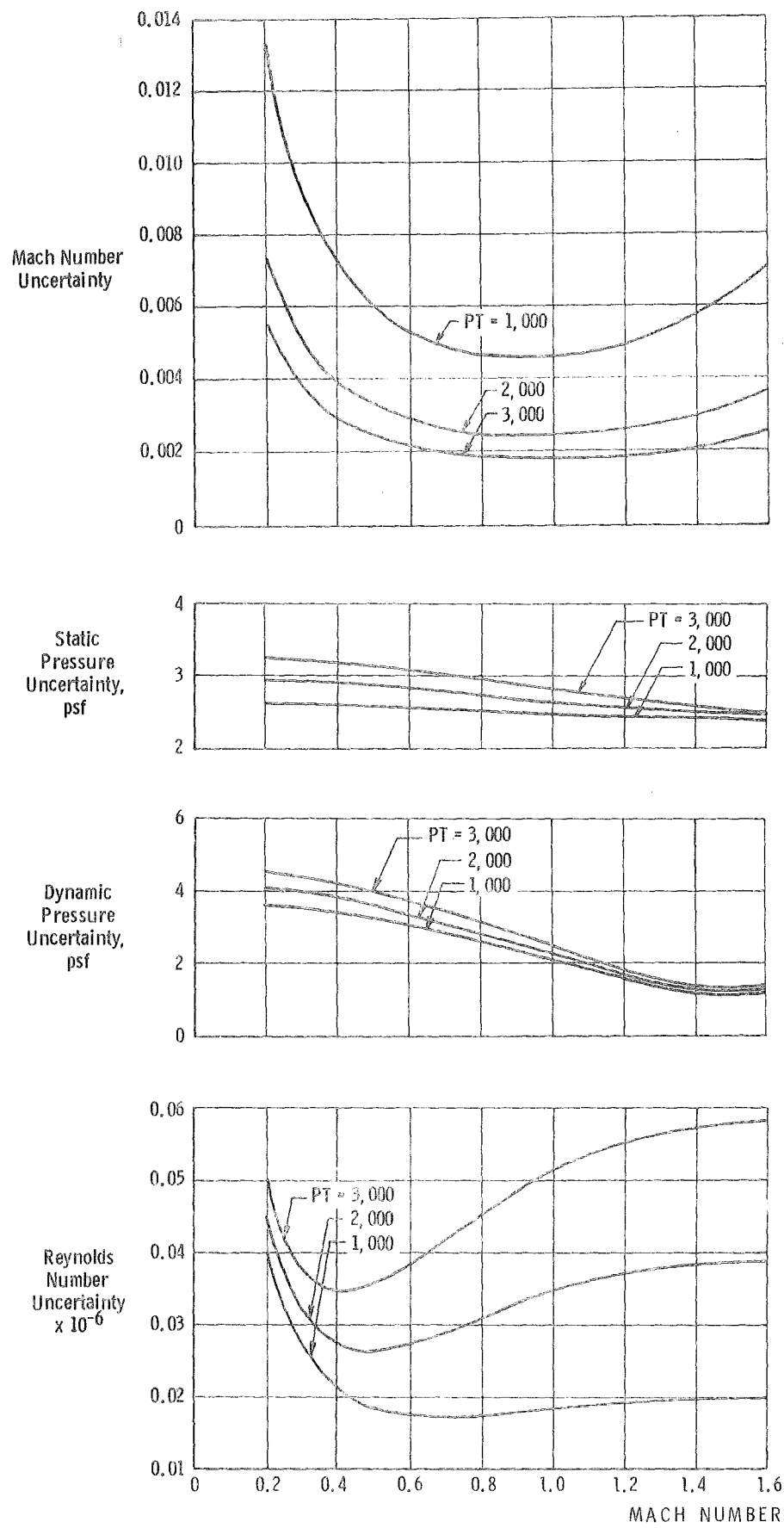


Figure 7. Estimated uncertainties in wind tunnel parameters.

Table 1

Pressure Orifice Locations

TAP - Pressure orifice number

MS - Model station, in.

X/L - Model station ratioed to model length(130.053 in.)

R - Model radius, in.

θ - Radial position, deg.

TAP	MS	X/L	R	θ
402	1.231	0.0095	0.4837	90
102	2.340	0.0180	0.9033	0
302	↓	↓	↓	180
203	3.380	0.0260	1.2775	270
103	4.222	0.0325	1.5646	0
403	4.972	0.0382	1.8067	90
104	5.673	0.0436	2.0199	0
204	6.384	0.0488	2.2127	270
105	7.013	0.0539	2.3900	0
305	↓	↓	↓	180
404	7.677	0.0590	2.5551	90
106	8.349	0.0642	2.7101	0
306	↓	↓	↓	180
205	9.036	0.0695	2.8667	270
107	9.741	0.0749	2.9961	0
307	↓	↓	↓	180
206	10.469	0.0805	3.1294	270
406	↓	↓	↓	90
108	11.222	0.0863	3.2571	0
308	↓	↓	↓	180
207	12.000	0.0923	3.3801	270
109	12.801	0.0984	3.4987	0
309	↓	↓	↓	180
407	13.624	0.1048	3.6134	90
110	14.468	0.1112	3.7246	0
208	15.327	0.1179	3.8326	270
408	↓	↓	↓	90
111	16.199	0.1246	3.9377	0
311	↓	↓	↓	180
209	17.082	0.1313	4.0399	270
409	↓	↓	↓	90
112	17.963	0.1381	4.1397	0

TAP	MS	X/L	R	θ
312	17.963	0.1381	4.1397	180
210	18.777	0.1444	4.2372	270
313	19.528	0.1502	4.3324	180
410	20.227	0.1555	4.4255	90
113	20.885	0.1606	4.5168	0
211	21.508	0.1654	4.6063	270
314	22.102	0.1699	4.6940	180
411	22.671	0.1743	4.7801	90
114	23.218	0.1785	4.8648	0
212	23.747	0.1826	4.9479	270
315	24.258	0.1865	5.0297	180
412	24.755	0.1903	5.1102	90
115	25.239	0.1941	5.1894	0
213	25.712	0.1977	5.2675	270
316	26.049	0.2003	5.3235	180
413	26.627	0.2047	5.4202	90
116	26.946	0.2072	5.4739	0
214	27.507	0.2115	5.5687	270
317	27.938	0.2148	5.6415	180
117	28.810	0.2215	5.7344	0
215	29.257	0.2250	5.8545	270
318	29.713	0.2285	5.9237	180
415	30.177	0.2320	5.9922	90
118	30.650	0.2357	6.0599	0
216	31.133	0.2394	6.1270	270
319	31.625	0.2432	6.1932	180
416	32.130	0.2471	6.2587	90
113	32.646	0.2510	6.3235	0
217	33.175	0.2551	6.3877	270
320	33.717	0.2593	6.4513	180
417	34.273	0.2635	6.5142	90
120	34.844	0.2679	6.5766	0

Table 3
Measurement Uncertainties

Parameter	M=0.6 TTR=565°R	M=0.9 TTR=570°R	M=1.2 TTR=575°R	M=1.5 TTR=580°R
	Uncertainty			
PRES, psia	±0.0460	±0.0370	±0.0320	±0.0300
COEF	±0.0063	±0.0037	±0.0027	±0.0022
CAPT	±0.0001	±0.0001	±0.0005	±0.0003
CA	±0.0019	±0.0013	±0.0013	±0.0011
CFB	±0.0019	±0.0014	±0.0011	±0.0010
CFGAGE	±0.0004	±0.0005	±0.0003	±0.0003
CFG	±0.0069	±0.0073	±0.0060	±0.0058

Note: Data uncertainty values are presented at a Reynolds number of $3.35 \times 10^6/\text{ft.}$

Table 4
Test Program Summary

M	REX10-6 1/ft	TTR °R	RUN NUMBERS		
			RAKES ON	RAKES OFF	
				DRY	WET
0.6	1.50	565	35	67, 80, 104	
	2.25		37	71	-
	3.35	↓	39, 54	74	101
		570	-	107, 109	-
		580	-	111, 113	-
		↓	585	-	-
	5.00	565	42	77	-
0.9	3.35	570	44	83	98
1.2		575	47	86	95
1.5	↓	580	51	89	92

DATE, 10-8-79 PROJECT NO. P41T-A2
 ARO, INC.
 AEDC DIVISION
 A SVERDRUP CORPORATION COMPANY
 PROPULSION WIND TUNNEL
 ARNOLD AIR FORCE STATION, TENNESSEE

Table 5

Summary of Test Data

TEST 547 ***** P41T-A2 TRANSONIC FLOW SKIN FRICTION TF-547 *****												AEDC PROPULSION WIND TUNNEL TRANSONIC 16T					
PIN	PIN	MACH	REX10-6	PT	P	Q	TTR	T8	SHX10-3	CAPFT	CAPAT	CCAV	CAPT	CA	CFB	CFRM	CFG
32.	1.	0.00	0.01	2051.4	2051.4	0.0	539.1	0.0	2.286	0.0	0.0	0.0	0.0	0.0	0.0	0.0	
35.	1.	0.60	1.50	972.3	763.7	190.9	565.9	557.0	2.976	0.00718	0.02170	0.04638	-0.01751	0.05417	0.07167	0.07010	
35.	2.	0.60	1.50	968.7	760.5	190.5	564.8	557.1	2.913	-0.00558	0.03476	0.04127	-0.01211	0.05421	0.06632	0.07010	
37.	1.	0.60	2.24	1451.8	1139.9	285.4	564.6	557.9	1.845	-0.00401	0.03453	0.04196	-0.01144	0.04948	0.06092	0.06588	
37.	2.	0.60	2.25	1455.6	1143.1	286.0	564.7	557.9	1.768	0.00302	0.02239	0.04706	-0.02165	0.04930	0.07095	0.06586	
39.	1.	0.60	3.35	2165.3	1698.8	426.8	564.4	558.2	7.059	-0.00703	0.03249	0.04431	-0.01884	0.04715	0.06599	0.06202	
39.	2.	0.60	3.35	2163.3	1696.7	426.9	564.3	558.1	7.393	0.00943	0.02492	0.04626	-0.01190	0.04694	0.05848	0.06202	
42.	1.	0.60	5.01	3230.8	2529.1	641.4	564.9	559.3	4.320	0.00109	0.03010	0.04478	-0.01359	0.04620	0.05979	0.056169	
42.	2.	0.60	5.01	3232.0	2529.7	642.0	565.2	559.4	4.031	0.00294	0.03487	0.04381	-0.00601	0.04592	0.05193	0.05845	
44.	1.	0.90	3.36	1748.7	1033.6	586.5	569.8	558.4	3.216	0.00862	0.03171	0.05832	-0.01799	0.04206	0.06005	0.05970	
44.	2.	0.90	3.35	1742.8	1030.5	584.2	569.5	558.4	3.167	0.00778	0.03573	0.05656	-0.01305	0.04214	0.05519	0.05707	
47.	1.	1.20	3.34	1661.5	683.7	691.1	575.6	558.3	0.910	0.07568	0.14075	0.20357	0.25765	0.05408	0.05692	0.05302	
47.	2.	1.20	3.34	1660.9	684.2	690.6	575.3	558.3	0.840	0.07584	0.14063	0.01277	0.20369	0.25796	0.05426	0.05211	
51.	1.	1.50	3.35	1742.6	747.2	747.7	580.1	557.6	0.505	0.08390	0.11302	0.00171	0.19521	0.24391	0.04870	0.05386	
51.	2.	1.50	3.35	1739.4	474.3	746.3	579.8	557.6	0.495	0.08396	0.11296	0.00134	0.19558	0.24415	0.04857	0.05387	
54.	1.	0.60	3.34	2165.5	1698.3	427.4	565.3	559.0	0.398	0.00305	0.02747	0.04555	-0.01503	0.04612	0.06115	0.06203	
54.	3.	0.60	3.35	2165.8	1697.2	428.5	565.5	559.1	0.396	0.00498	0.02704	0.04489	-0.01287	0.04597	0.05884	0.06202	
60.	1.	0.01	0.05	2050.8	2050.7	0.1	555.1	0.0	0.876	0.0	0.0	0.0	0.0	0.0	0.0	0.0	
67.	1.	0.60	1.49	968.2	760.7	189.9	564.4	556.8	1.947	0.00131	0.02864	0.04322	-0.01326	0.05493	0.06819	0.07012	
67.	2.	0.60	1.50	970.4	762.2	190.6	564.3	556.9	1.953	0.00493	0.02501	0.04489	-0.01494	0.05451	0.06945	0.07008	
71.	1.	0.60	2.25	1454.4	1141.1	286.7	564.7	557.2	1.363	0.00117	0.02768	0.04448	-0.01562	0.04985	0.06547	0.06445	
71.	2.	0.60	2.24	1453.2	1140.7	286.0	564.6	557.3	1.372	0.00264	0.02869	0.04421	-0.01288	0.04980	0.06268	0.06588	
74.	1.	0.60	3.35	2164.8	1696.4	428.3	564.8	558.2	1.487	-0.00215	0.03406	0.04285	-0.01094	0.04614	0.05708	0.06201	
74.	2.	0.60	3.35	2165.1	1697.3	427.9	564.8	558.1	1.451	0.00126	0.03104	0.04428	-0.01157	0.04615	0.05812	0.06201	
77.	1.	0.60	5.01	3230.2	2528.7	641.3	564.6	559.0	3.334	-0.00451	0.03361	0.04346	-0.01435	0.04477	0.05913	0.05396	
77.	2.	0.60	5.01	3229.3	2528.3	640.9	564.6	559.0	3.207	0.00588	0.02937	0.04463	-0.00938	0.04490	0.05428	0.05391	
80.	1.	0.60	1.49	968.6	760.6	190.4	565.4	557.1	1.473	-0.00355	0.03355	0.04147	-0.01147	0.05340	0.06487	0.07012	
80.	2.	0.60	1.49	969.5	761.4	190.5	565.4	557.1	1.388	0.00193	0.02731	0.04382	-0.01458	0.05303	0.06761	0.07012	
83.	1.	0.90	3.36	1744.9	1031.5	585.1	568.8	558.4	0.674	0.00893	0.03159	0.05797	-0.01745	0.03940	0.05685	0.05971	
83.	2.	0.90	3.36	1749.3	1034.6	586.3	569.3	558.4	0.658	0.00891	0.03026	0.05881	-0.01964	0.03917	0.05881	0.05548	
86.	1.	1.20	3.35	1663.0	684.5	691.6	574.7	558.3	0.813	0.07477	0.14159	0.01401	0.20236	0.25334	0.05098	0.05690	
86.	2.	1.20	3.35	1661.5	684.1	690.9	574.6	558.2	0.788	0.07296	0.14298	0.01324	0.20269	0.25364	0.05094	0.05690	
89.	1.	1.50	3.35	1738.5	473.2	745.8	579.1	558.2	0.575	0.08211	0.11470	0.00159	0.19522	0.24110	0.04588	0.05385	
89.	2.	1.50	3.35	1738.6	474.1	746.0	579.2	558.1	0.547	0.08381	0.11343	0.00212	0.19512	0.23984	0.04471	0.05386	
92.	1.	1.50	3.35	1740.1	473.6	746.5	580.0	557.9	1.175	0.08465	0.11386	0.00192	0.19659	0.24114	0.04455	0.05386	
95.	1.	1.20	3.35	1660.0	683.4	690.4	574.7	557.9	5.859	0.07833	0.13340	0.01732	0.19441	0.24541	0.05100	0.05691	
98.	1.	0.90	3.36	1742.1	1033.1	586.4	569.5	558.6	7.969	0.00771	0.03112	0.05858	-0.01975	0.03984	0.05959	0.05970	
101.	1.	0.60	3.36	2164.8	1696.3	428.4	564.0	558.8	8.517	0.00437	0.03222	0.04358	-0.00699	0.04654	0.05353	0.06655	
104.	1.	0.60	1.49	968.4	760.9	189.9	565.3	557.7	8.850	-0.00007	0.02948	0.04296	-0.01356	0.05451	0.06807	0.07014	
107.	1.	0.60	3.35	2188.9	1716.2	432.3	569.9	560.8	9.724	-0.00435	0.03662	0.04180	-0.00953	0.04713	0.05666	0.06202	
107.	2.	0.60	3.36	2193.0	1718.3	434.1	569.9	561.2	9.706	0.00220	0.02891	0.04504	-0.01394	0.04690	0.06083	0.06199	
107.	3.	0.60	3.36	2190.8	1716.6	433.6	569.6	561.7	9.716	0.00225	0.03117	0.04402	-0.01063	0.04671	0.05734	0.06199	
107.	4.	0.60	3.36	2191.8	1717.7	433.6	569.6	562.0	9.676	0.00244	0.02798	0.04535	-0.01494	0.04680	0.06174	0.06199	
107.	5.	0.60	3.35	2189.0	1715.7	432.8	569.9	562.3	9.688	-0.00007	0.03123	0.04416	-0.01300	0.04681	0.05981	0.06201	
107.	6.	0.60	3.36	2193.2	1719.0	433.7	569.9	562.4	9.670	-0.00156	0.02826	0.04532	-0.01862	0.04698	0.06560	0.06200	
109.	2.	0.60	3.36	2192.5	1718.8	433.3	569.6	562.9	9.637	0.00565	0.02478	0.04605	-0.01562	0.04669	0.06231	0.06200	
111.	1.	0.60	3.35	2240.8	1756.5	442.9	580.4	566.0	9.671	0.00311	0.02843	0.04545	-0.01392	0.04682	0.06074	0.06201	
111.	2.	0.60	3.36	2242.1	1757.1	443.6	579.4	566.9	9.685	0.00241	0.02957	0.04479	-0.01280	0.04665	0.05964	0.06198	
111.	3.	0.60	3.35	2239.1	1755.9	442.0	579.7	567.7	9.678	-0.00134	0.03060	0.04430	-0.01050	0.04708	0.06213	0.06202	
111.	4.	0.60	3.35	2237.7	1753.1	443.1	579.7	568.5	9.684	0.00139	0.02956	0.04438	-0.01342	0.04670	0.06013	0.06200	
111.	5.	0.60	3.35	2243.3	1757.5	444.3	581.7	569.2	9.660	0.00501	0.02537	0.04555	-0.01517	0.04659	0.06176	0.06202	
111.	6.	0.60	3.32	2240.9	1756.4	443.1	584.5	570.4	9.670	0.00729	0.02660	0.04574	-0.01185	0.04663	0.05848	0.06209	
111.	8.	0.60	3.32	2243.4	1758.6	443.4	585.1	572.0	9.695	0.00434	0.02562	0.04590	-0.01593	0.04661	0.06254	0.06210	
111.	9.	0.60	3.32	2241.1	1755.9	443.7	585.0	572.9	9.669	0.00303	0.02981	0.04394	-0.01029	0.04664	0.05693	0.06209	
113.	1.	0.60	3.36	2240.0	1755.8	442.8	579.2	572.7	9.674	0.00308	0.02843	0.04489	-0.01339	0.04633	0.05972	0.06199	

Table 6

NOMENCLATURE FOR
SUMMARY OF TEST DATA

RN	Data run number (a data subset containing variations of only one independent parameter)
PN	Data point number (a single record of all test parameters)
MACH	Free-stream Mach number
REX10-6	Free-stream unit Reynolds number $\times 10^{-6}$, 1/ft
PT	Free-stream total pressure, psfa
P	Free-stream static pressure, psfa
Q	Free-stream dynamic pressure, psf
TTR	Free-stream total temperature, °R
T8	Model surface temperature at $X/L = 0.538$ (X is the distance from the model nose in inches and L is the model length, 130.053 in.), °R
SHX10+3	Tunnel specific humidity $\times 10^{+3}$
CAPFT	Integrated pressure force coefficient of forebody ($X/L = 0.0$ to $X/L = 0.505$), positive aft
CAPAT	Integrated pressure force coefficient of after-body ($X/L = 0.505$ to $X/L = 1.0$), positive aft
CCAV	Model cavity pressure force coefficient, positive forward, $FCAV/Q(1.4243 \text{ ft}^2)$
CAPT	Total integrated pressure force coefficient including cavity pressure contribution, positive aft, $CAPFT + CAPAT - CCAV$
CA	Balance measured total drag coefficient, $FA/Q(1.4243 \text{ ft}^2)$
CFB	Skin friction drag coefficient calculated from balance and pressure data, $CA - CAPT$

Table 6
Concluded

CFRM Skin friction drag coefficient calculated
from Mach number and Reynolds number

CFG Skin friction drag coefficient calculated
from integrated wire gage data, SF/Q(1.4243 ft²)

APPENDIX
WIRE GAGE DATA REDUCTION EQUATIONS

1. For Each Gage:

Local Skin Friction Force per Unit Area

$$SFGAGE = \frac{32.2 (MU)^2}{RHO} \left[\frac{1}{A} (ISR-B) \right]^3, \text{ lb/ft}^2$$

where:

$$MU = 2.27 \times 10^{-8} \frac{TG^{1.5}}{TG+198.6}, \text{ lb-sec/ft}^2$$

$$RHO = \frac{144 (PXXX)}{53.35 (TG)}, \text{ lbm/ft}^3$$

$$ISR = \frac{(VGAGE) (IGAGE)}{RHOT - RCOLD}, \text{ watts/ohm}$$

$$TG = (KA) (RHOT) + (KB) + 460, \text{ }^{\circ}\text{R}$$

Notes: KA, KB, A, and B are constants.

RHOT and RCOLD are ratios of VGAGE and IGAGE.

Correlation Between Gage Number and Local Static Pressure Number

GAGE	PXXX										
2	P303	8	P311	14	P317	20	P222	28	P329	35	P134
3	P304	9	P312	15	P415	23	P531	30	P636	36	P335
4	P404	10	P410	16	P416	24	P126	31	P331	37	P336
5	P307	11	P314	18	P122	26	P634	32	P332	38	P438
7	P407	12	P212	19	P221	27	P128	34	P433	39	P241
											40 P445

2. Integrated Skin Friction Drag:

$$SF = \sum_{i=2}^{i=40} \left\{ \left[\frac{SFGAGE_i + SFGAGE_{i-1}}{2} \right] (\cos \theta_i) A_i \right\}, \text{ lb}$$